ACS APPLIED MATERIALS & INTERFACES

Research Article

www.acsami.org

A New, High Energy Sn−C/Li[$Li_{0.2}Ni_{0.4/3}Co_{0.4/3}Mn_{1.6/3}$]$O_2$ Lithium-Ion Battery

Giuseppe Antonio Elia,[†] Jun Wang,[‡] Dominic Bresser,[‡] Jie Li,[‡] Bruno Scrosati,[§,∥] Stefano Passerini,*[,‡,∥] and Jusef Hassoun[†,*]

[†]Chemistry Department, Sapienza University of Rome, Piazzale Aldo Moro 5, 00185, Rome, Italy

[‡]Institute of Physical Chemistry & MEET Battery Research Centre, University of Muenster, Corrensstrasse 28/30 & 46, 48149 Muenster, Germany

[§]Italian Institute of Technology (IIT), Genova, Italy

[∥]Helmholtz-Institute Ulm, Karlsruher Institute of Technology, Albert-Einstein-Allee 11, 89081 Ulm, Germany

ABSTRACT: In this paper we report a new, high performance lithium-ion battery comprising a nanostructured Sn−C anode and Li[$Li_{0.2}Ni_{0.4/3}Co_{0.4/3}Mn_{1.6/3}$]$O_2$ (lithium-rich) cathode. This battery shows highly promising long-term cycling stability for up to 500 cycles, excellent rate capability, and a practical energy density, which is expected to be as high as 220 Wh kg^{-1} at the packaged cell level. Considering the overall performance of this new chemistry basically related to the optimized structure, morphology, and composition of the utilized active materials as demonstrated by XRD, TEM, and SEM, respectively, the system studied herein is proposed as a suitable candidate for application in the lithium-ion battery field.

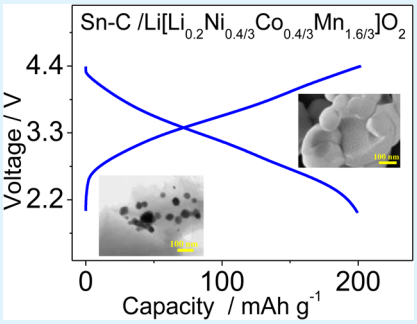

KEYWORDS: *nanostructured Sn−C, lithium-rich cathode, long life, lithium-ion battery*

INTRODUCTION

Severe economy and climate changes within recent years triggered large demand for secure, clean, and efficient energy resources, resulting in a remarkable development of renewable energy supply and (hybrid) electric vehicles. However, the proper use of renewable energy requires its efficient storage. Accordingly, lithium-ion batteries have attracted substantial interest as versatile, safe, and clean energy storage devices. Consequently, they are presently considered as the power source of choice for (hybrid) electric vehicles and as supply/demand-balancing energy storage for renewable energy plants. The currently leading, conventional, and mostly utilized lithium-ion battery differs only little from the first lithium-ion battery developed by Sony in the early 1990s,[1] which comprised graphite, lithium cobalt oxide, and an organic carbonate-based solution containing a lithium salt as the anode, cathode, and electrolyte, respectively. However, enabling, for instance, electric vehicles with a convenient driving range and safety characteristics requires the improvement of the energy density and the development and implementation of safer electrolytes in order to reduce the safety issues generally related to these high energy systems.[2,3] For such reasons, researchers are investigating alternative electrode active materials enabling increased specific capacities and/or higher operational voltages to increase the energy density and specific energy of such devices. Regarding the anode side, lithium−metal alloys, such as Li−Sn and Li−Si, are currently considered as the most appealing active materials,[4] in particular in their most advanced, nanostructured configuration, frequently leading to enhanced cycling stabilities and specific capacities ranging from 400 to 2000 mAh g^{-1}(vs 372 mAh $g^{-1}$for the state-of-the-art anode material graphite).[5,6]With respect to the cathode side, solid-solution layered oxides, such as the combination of Li_2MnO_3 and $LiMO_2$ (M = Mn, Co, Ni, etc.), are attracting increasing interest as suitable cathode materials due to their superior electrochemical, chemical, and thermal stability, and, in particular, due to their enhanced specific capacities in comparison with $LiCoO_2$. Moreover, the possibility of partially or even completely replacing toxic and expensive cobalt with more sustainable transition metals has led to a substantial interest in this class of active materials.[7−9] We demonstrated recently that the lithium-rich active material with the general formula Li[$Li_{1/3}Mn_{2/3}$]O_2 × $LiMO_2$(M = Mn, Ni, Co) is a suitable candidate for next generation lithium-ion batteries because of its superior specific capacity, enhanced rate capability, and stable cycling performance.[10,11] In addition, we reported a nanostructured Sn−C composite, showing higher specific capacities and greater rate capability than the state-of-the-art lithium-ion anode material, graphite.[12]

Herein, we report the combination of the high performance Li[$Li_{0.2}Ni_{0.4/3}Co_{0.4/3}Mn_{1.6/3}$]$O_2$ and nanostructured Sn−C electrodes in a lithium-ion battery showing excellent electro-

Received: May 10, 2014
Accepted: July 11, 2014
Published: July 11, 2014

chemical performance in terms of cycle life, rate capability, and energy density. Accordingly, we propose this new electrode chemistry combination as a suitable candidate for application in efficient energy storage systems.

EXPERIMENTAL SECTION

The synthesis of the Sn−C nanocomposite, involving a resorcinol−formaldehyde gel preparation and impregnation with an organometallic tin precursor, followed by annealing under argon−hydrogen atmosphere, was reported already in previous studies.[13,14] Thermogravimetric analysis (TGA) was performed on the Sn−C composite in the temperature range 25−950 °C under air flux (60 mL min^{-1}) applying a heating rate of 10 °C min^{-1}. The synthesis of the lithium-rich cathode $Li[Li_{0.2}Ni_{0.4/3}Co_{0.4/3}Mn_{1.6/3}]O_2$ material was reported recently in detail by Wang et al.[10,11] Briefly, $Li[Li_{0.2}Ni_{0.4/3}Co_{0.4/3}Mn_{1.6/3}]O_2$ was prepared by coprecipitation of nickel, cobalt, and manganese acetate (Aldrich, >98%) in a molar ratio of 1:1:4 with lithium hydroxide hydrate (Aldrich, >98%) in an aqueous solution. The precipitate was rinsed extensively with distilled water and, then, dried at 120 °C under vacuum overnight. Subsequently, this precursor was mixed with lithium carbonate (Aldrich, >98%), and the resulting mixture was annealed in two steps at 500 °C for 5 h and at 850 °C for 20 h under air.

The structure of the synthesized active materials was analyzed by using either a Rigaku D-Max X-ray diffraction (XRD) instrument or a Bruker D8 Advance, both equipped with a Cu $K\alpha_1$ radiation source. The morphology of the lithium-rich cathode powder was investigated by using a scanning electron microscope (SEM, ZEISS AURIGA), while the morphology of the Sn−C anode powder was studied by means of transmission electron microscopy (TEM, JEOL 1200EX II microscope) and scanning electron microscopy (SEM Phenom-Fei). For the electrochemical characterization, electrodes were prepared by casting a slurry, comprising 80 wt % active material, 10 wt % PVdF (6020 Solef Solvay, binder), and 10 wt % SP C-65 (Timcal, electron conducting additive) dispersed in *N*-methyl-2-pyrrolidone (NMP, Aldrich), on copper (for Sn−C) and aluminum (for $Li[Li_{0.2}Ni_{0.4/3}Co_{0.4/3}Mn_{1.6/3}]O_2$) foils using a laboratory-scale doctor blade. These electrode tapes were subsequently dried in an oven at 60 °C. The electrodes disks having a diameter of 12 mm were punched and dried again under vacuum at 110 °C overnight. The active material mass loading was on the order of 1 mg cm^{-2} for the anode and about 1.5 mg cm^{-2} for the cathode. The electrochemical characterization was performed using three-electrode Swagelok-type cells. In lithium-ion half-cells the Sn−C and the $Li[Li_{0.2}Ni_{0.4/3}Co_{0.4/3}Mn_{1.6/3}]O_2$ electrodes were used as the working electrodes, while metal lithium disks were utilized as counter and reference electrode. A layer of glass fiber (Whatman) soaked with a 1M solution of $LiPF_6$ in EC:DEC 3:7 was used as the electrolyte. The cells were assembled in an argon-filled drybox with an O_2 and H_2O content lower than 1 ppm. Galvanostatic cycling tests within the voltage range 0.01−2 V for Sn−C and 2.5−4.7 V for $Li[Li_{0.2}Ni_{0.4/3}Co_{0.4/3}Mn_{1.6/3}]O_2$ were carried out by means of a Maccor Series 4000 Battery Test System. Cyclic voltammetry was performed in the same potential ranges using a scan rate of 0.1 mV s^{-1} by means of a VMP2/Z multichannel galvanostat−potentiostat (Bio-Logic, France). Prior to full-cell assembly and cycling, the irreversible capacity of the Sn−C anode was limited by a chemical activation procedure. This consisted of placing in contact the anode and a lithium foil wetted by 1M solution of $LiPF_6$ in EC:DEC for 10 min using a pressure of 0.2 kg cm^{-2}, as reported in a previous publication.[12] The galvanostatic cycling of the cathode-limited lithium-ion cell was conducted by means of a VMP2/Z multichannel galvanostat−potentiostat (Bio-Logic, France) in the 2−4.4 V range, using a procedure consisting of the repetition of a series of increasing C-rates, corresponding to a specific current of 100, 200, and 300 mA g^{-1}, for up to 500 cycles. All electrochemical studies were performed at room temperature.

RESULTS AND DISCUSSION

Prior to its electrochemical characterization, the anode and cathode active materials were structurally and morphologically characterized by XRD and SEM/TEM analysis. The diffraction pattern reported in Figure 1a shows reflections that can be

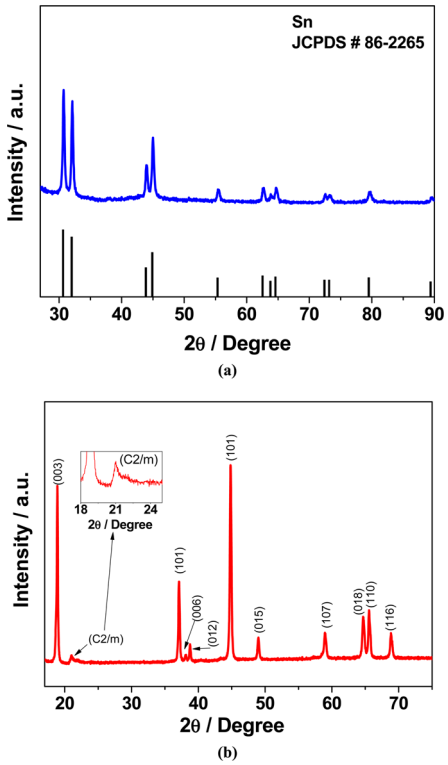

Figure 1. XRD patterns of the Sn−C nanostructured composite anode (a) and of the $Li[Li_{0.2}Ni_{0.4/3}Co_{0.4/3}Mn_{1.6/3}]O_2$ cathode (b); in the inset is the magnification of the *C*2/*m* phase reflection peak.

assigned to metallic Sn (JCPDS no. 86-2265), while no evidence of SnO or SnO_2 was detected, revealing proper synthesis conditions. The presence of metallic tin, only, is expected to result in a superior electrochemical performance of the active material both in terms of high capacity retention and low charge−discharge polarization.[13,14] In Figure 1b, the diffraction pattern obtained for $Li[Li_{0.2}Ni_{0.4/3}Co_{0.4/3}Mn_{1.6/3}]O_2$ shows the well-defined α-$NaFeO_2$-type structure, with a $R\bar{3}m$ space group and, in minor part, with a *C*2/*m* space group as indicated by the low intensity reflections magnified in the figure inset at about $2\theta = 21°$.[15,16] According to previous experience with these two active materials, these structural characteristics are expected to result in the optimum electrochemical performance when applied as anode and cathode in a lithium-ion cell.

Figure 2a, reporting the TG analysis of the Sn−C composite, reveals a Sn:C weight ratio of about 38:62. The morphology of the Sn−C and $Li[Li_{0.2}Ni_{0.4/3}Co_{0.4/3}Mn_{1.6/3}]O_2$ samples was studied by TEM and SEM, respectively. The SEM image of the Sn−C reported in Figure 2b shows micrometric morphology of the composite, i.e., having a particle size of about 50−60 μm, while the TEM images reported in Figure 2c and 2d evidence that the amorphous carbon matrix is uniformly loaded by Sn particles with a size of few tens of nanometers. This morphology ensures contemporarily high tap-density and, thus, high volumetric energy density, as well as optimized

dx.doi.org/10.1021/am502884y | ACS Appl. Mater. Interfaces 2014, 6, 12956−12961

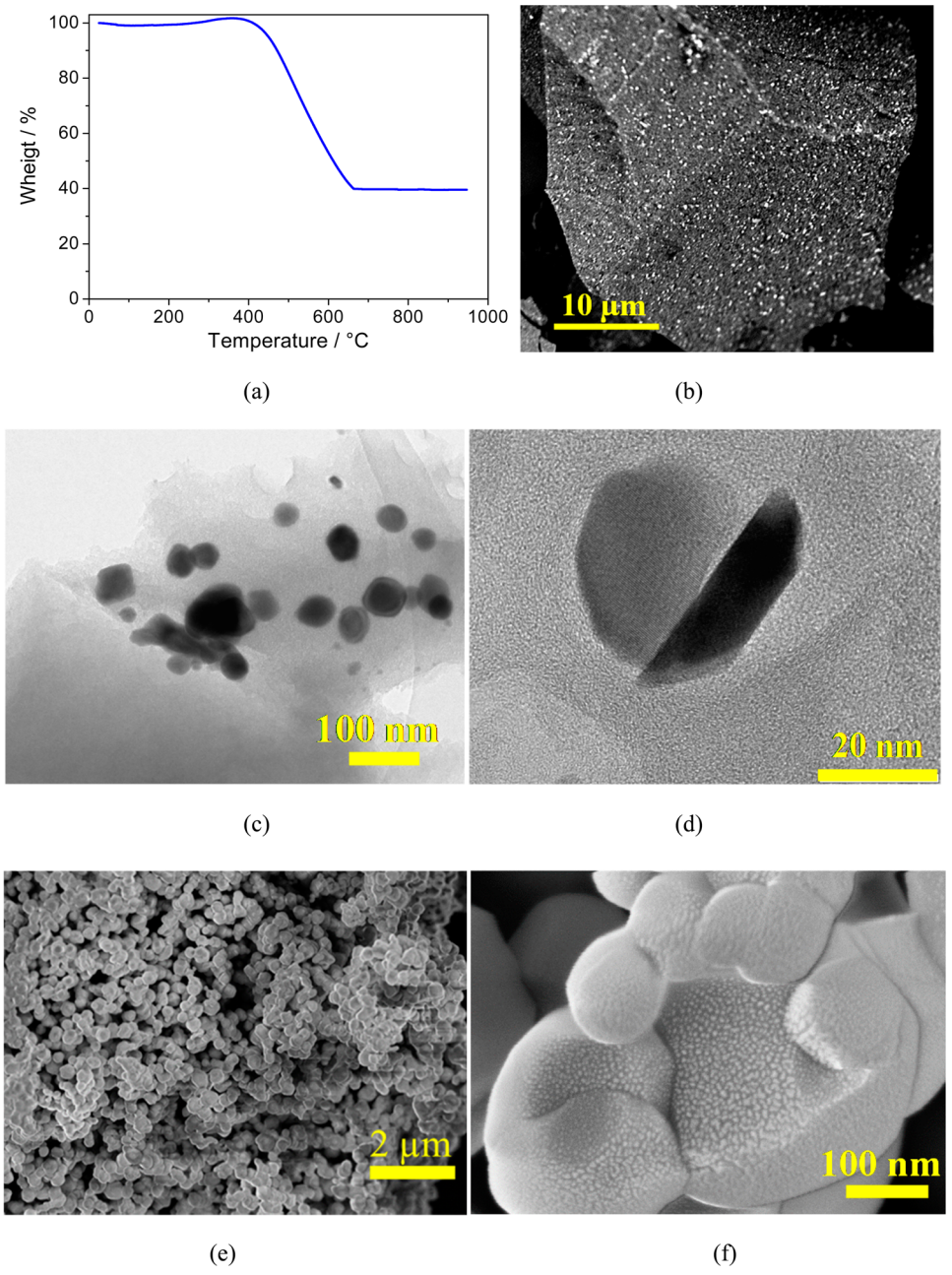

Figure 2. (a) TG analysis of the Sn−C composite performed under air, (b) SEM image of the Sn−C anode, (c and d) TEM images at various magnifications of the Sn−C nanostructured composite, and (e and f) SEM images at various magnifications of the $Li[Li_{0.2}Ni_{0.4/3}Co_{0.4/3}Mn_{1.6/3}]O_2$ cathode material.

cycling performance due to the reduction of the mechanical stress affecting the nanostructured Sn particles upon electrochemical (de-)alloying process. Moreover, this peculiar morphology determines further relevant aspects of the electrochemical behavior, such as the initial irreversible capacity associated with the reduced surface area by utilizing micrometer-sized rather than nanosized particles, resulting in a reduced initial electrolyte decomposition, i.e., a decreased solid electrolyte interphase (SEI) formation. Regarding the reversible lithium storage in the carbon matrix, previous studies evidenced a contribution of about 100 mAh g^{-1} to the overall reversible capacity.[13,14] Hence, considering the Sn to C weight ratio of 38:62 and the corresponding specific capacities of 993 mAh g^{-1} and 100 mAh g^{-1} for Sn and carbon, respectively, the composite is expected to deliver a reversible capacity of about 440 mAh g^{-1}.

Figure 2e and f, showing the SEM images of the $Li[Li_{0.2}Ni_{0.4/3}Co_{0.4/3}Mn_{1.6/3}]O_2$ layered cathode, reveal that this material is composed of aggregates of primary particles, having an average diameter of about 100−200 nm. This particular morphology, studied in detail in the literature,[17] allows short diffusion pathways for lithium ion diffusion, resulting in an improved electrochemical performance, particularly at elevated (dis-)charge rates. In addition, the formation of larger secondary particles leads to a reduced surface area, limiting the occurrence of side reactions during the electrode charge process.[18,19]

Figure 3a compares the cyclic voltammetry profiles of the Sn−C anode and the $Li[Li_{0.2}Ni_{0.4/3}Co_{0.4/3}Mn_{1.6/3}]O_2$ cathode.

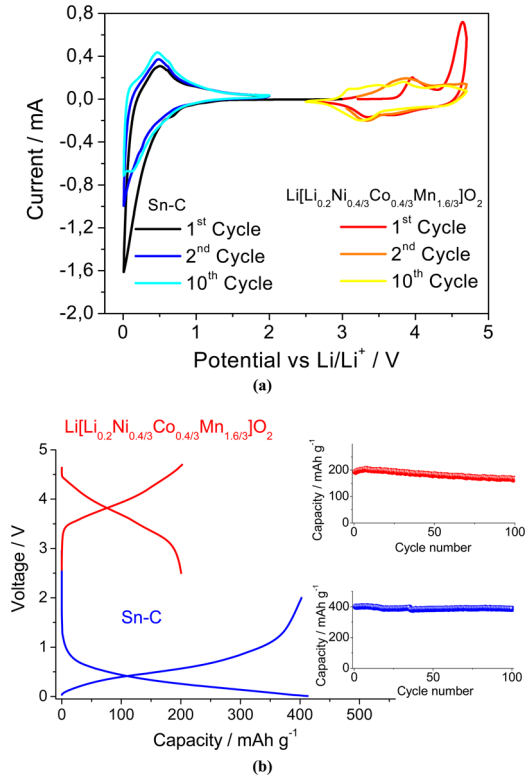

Figure 3. (a) Cyclic voltammetry at a scan rate of 0.1 mV s^{-1} of the Sn−C composite (left, potential window of 0.01−2 V) and $Li[Li_{0.2}Ni_{0.4/3}Co_{0.4/3}Mn_{1.6/3}]O_2$ (right curve, potential window of 2.5−4.7 V) electrodes. (b) Voltage profiles recorded at the fifth cycle of lithium-ion half-cells comprising the Sn−C nanocomposite (blue, voltage range 0.01 to 2.0 V) or the $Li[Li_{0.2}Ni_{0.4/3}Co_{0.4/3}Mn_{1.6/3}]O_2$ cathode (red, voltage range 2.5 to 4.7 V), applying a specific current of 100 mA g^{-1}. In the insets the long-term cycling performance for these half-cells is presented.

During the first scan, the Sn−C curve (reported in black) shows the typical irreversible processes related to the SEI formation on the amorphous carbon matrix and the reduction of synthesis residuals,[13,20] while the following cycles are characterized by the expected reversible profile, associated with the lithium−tin alloying/dealloying process, centered at about 0.5 V vs Li/Li^+.[21,22] Meanwhile, the $Li[Li_{0.2}Ni_{0.4/3}Co_{0.4/3}Mn_{1.6/3}]O_2$ cathode profile shows during the first charge (reported in red) the irreversible oxidation peak around 4.5−4.7 V associated with a structural reorganization of the electrode and associated partial oxygen loss, typical of this class of materials.[23] The subsequent voltammetric cycle shows peaks associated with the reversible insertion/extraction of lithium into the octahedral site of the layered structure centered at potential values of 3.9 and 3.4 V upon oxidation and reduction, respectively.[24,25] Furthermore, a shift of the reversible oxidation process to lower potential values, i.e., around 3.0 V, caused by the structural layered/spinel intergrowth in the electrode structure,[26] is observed for the following cycles. Figure 3b shows the steady state voltage signature of the Sn−C anode (blue curve) and of the $Li[Li_{0.2}Ni_{0.4/3}Co_{0.4/3}Mn_{1.6/3}]O_2$ cathode (red curve) upon galvanostatic cycling in lithium half-cells. In the inset, the corresponding long-term cycling performance for 100 continuous (dis-)charge cycles is presented. The figure reveals that the Sn−C anode delivers a stable capacity of about 400 mAh g^{-1}, i.e., a value approaching the theoretically expected specific capacity for this nanocomposite with an average operational potential of about 0.5 V and a capacity retention of around 98% after 100 cycles (see related inset in Figure 3b). The Sn−C voltage profile well reflects the lithium−tin alloying/dealloying process in a nanostructured compound, in which the multiplateau curve expected by the various alloying/dealloying steps is, instead, merged in one sloping profile.[14] Meanwhile, the voltage profile of the $Li[Li_{0.2}Ni_{0.4/3}Co_{0.4/3}Mn_{1.6/3}]O_2$ reported in Figure 3b shows the typical lithiation−delithiation process of NMC-layered electrodes characterized by a solid-solution-like behavior possibly accompanied by some phase changes during the electrochemical process that may lead to partial capacity fading, in particular upon continuous cycling. Figure 3 evidences that the $Li[Li_{0.2}Ni_{0.4/3}Co_{0.4/3}Mn_{1.6/3}]O_2$ discharge process starts at 4.5 V and proceeds almost linearly until 3.1 V, so that the average working voltage of the electrode is calculated to be 3.8 V, with a specific capacity of about 200 mAh g^{-1} and a capacity retention of 88% after 100 charge−discharge cycles (see related inset in Figure 3b). With respect to the electrode properties in terms of their average operational potentials, the full-cell adopting the Sn−C nanocomposite as anode and the lithium-rich $Li[Li_{0.2}Ni_{0.4/3}Co_{0.4/3}Mn_{1.6/3}]O_2$ as cathode active material is supposed to have an average working voltage of about 3.3 V, a specific capacity of 200 mAh g^{-1} (referred to the cathode mass), and, hence, a theoretical specific energy of about 660 Wh kg^{-1}.

The Sn−C anode and $Li[Li_{0.2}Ni_{0.4/3}Co_{0.4/3}Mn_{1.6/3}]O_2$ cathode were combined in a lithium-ion full-cell, and the performance is reported in Figure 4, both in terms of voltage profile (a) and cycling behavior (b) at different specific currents (100, 200, and 300 mA g^{-1}). The voltage profiles given in Figure 4a evidence that, following the first activation cycle (black curve), the cell voltage follows the expected reversible (de)lithiation reaction:

$$Sn{-}C + Li[Li_{0.2}Ni_{0.4/3}Co_{0.4/3}Mn_{1.6/3}]O_2 \leftrightarrow Li_xSn{-}C + Li_{(1-x)}[Li_{0.2}Ni_{0.4/3}Co_{0.4/3}Mn_{1.6/3}]O_2$$

Considering that the irreversible capacity of the Sn−C anode was reduced by chemically activating the electrode prior to the full-cell assembly[11] (see Experimental Section), the first cycle of the full-cell reflects well the partially irreversible feature of the $Li[Li_{0.2}Ni_{0.4/3}Co_{0.4/3}Mn_{1.6/3}]O_2$ cathode (Figure 4, compare also with Figure 3a). In the following, the overall process of the full-cell evolves through the expected reversible (de-)alloying process at the anode side, centered at about 0.5 V vs Li/Li^+, and the lithium (de-)intercalation process at the cathod, evolving at about 3.8 V vs Li/Li^+, with an average working voltage of 3.3 V and specific capacities ranging from 200 mAh g^{-1} at 100 mA g^{-1} (i.e., 2 h charge and discharge) to 175 mAh g^{-1} at 300 mA g^{-1} (35 min charge and discharge). Besides, it is observed that the capacity slightly increases upon the first few cycles, which is most likely related to some structural reorganization of the anode and cathode active material upon the initial (de-)lithiation cycles. Advantageously, the cell shows only a little increase in polarization for an increasing specific current, thus confirming the highly promising electrode properties due to the optimized structure and morphology of the utilized active materials. As a matter of fact, such cells show a remarkable cycle

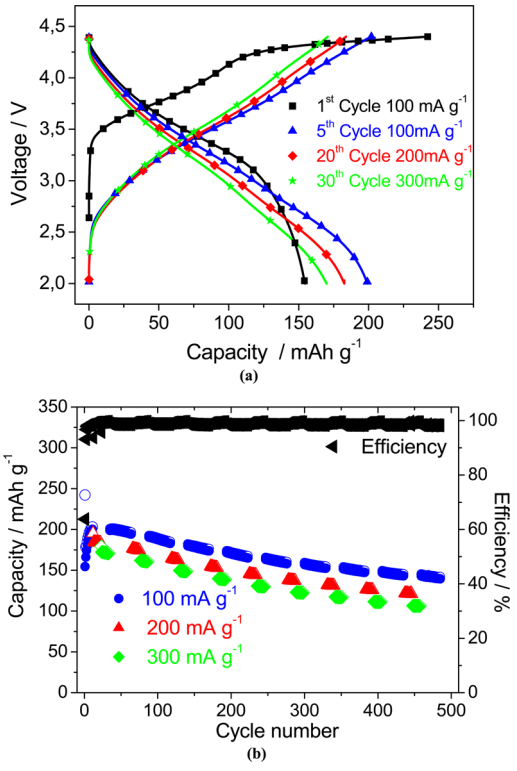

Figure 4. (a) Voltage profiles and (b) long-term cycling performance of the Sn−C/Li[$Li_{0.2}Ni_{0.4/3}Co_{0.4/3}Mn_{1.6/3}$]$O_2$ lithium-ion full-cell upon different specific currents (100, 200, 300 mA g^{-1}) within 2.0 and 4.4 V cutoff voltages.

life, delivering a stable capacity for up to 500 (dis-)charge cycles with a capacity retention of about 75% and a Coulombic efficiency of more than 99% (after the initial activation cycles) (Figure 4b). This stable cycling performance is considered remarkably high, in particular taking into account the cycling conditions involving a repeated series of increasing specific currents during the whole test.

CONCLUSIONS

The Sn−C/Li[$Li_{0.2}Ni_{0.4/3}Co_{0.4/3}Mn_{1.6/3}$]$O_2$ lithium-ion cell reported in this work involved high performance materials characterized by remarkable properties in terms of cycle life, rate capability, and delivered capacity, basically related to previously optimized structures and morphologies. This cell evidenced a very stable cycling performance for up to 500 cycles with maximum capacity of 200 mAh g^{-1} and an average operational voltage of 3.3 V, resulting in a theoretical energy density of about 660 Wh kg^{-1}, which is a value that competes well with that reported in literature for lithium-ion batteries of advanced configuration.[27] Considering also electrochemically inactive cell components such as, for instance, the cell casing, the electrolyte, and the current collector, the practical specific energy of the cell can be estimated to about 220 Wh kg^{-1}, i.e., a specific energy substantially higher than that of currently available state-of-the-art lithium-ion batteries. Thus, the herein presented lithium-ion chemistry appears highly promising for the realization of future high energy and high power lithium-ion batteries enabling electric vehicles with enhanced driving ranges and improved safety characteristics. It appears noteworthy that we focused this study on the suitability of the combination of the two electrodes for application in a lab-scale lithium-ion full-cell that, to the best of our knowledge, is originally reported herein. However, the upscaling of this system might raise additional issues such as, for instance, the large-scale material production, the practical battery stack assembly using multilayer pouch−cell configuration, and the proper electrode loading, as well as the electrolyte and separator selection.

AUTHOR INFORMATION

Corresponding Authors

*E-mail: jusef.hassoun@uniroma1.it (J.H.).
*E-mail: stefano.passerini@uni-muenster.de (S.P.).

Notes

The authors declare no competing financial interest.

ACKNOWLEDGMENTS

G.A.E., B.S., and J.H. acknowledge the support of the Italian Institute of Technology (Project "REALIST" *Rechargeable, advanced, nano structured lithium batteries with high energy* storage) and "Regione Lazio", Italy. J.W. and J.L. kindly acknowledge the financial support of the Federal Ministry of Education and Research, the Federal Ministry of Economics and Technology, as well as the Federal Ministry for the Environment, Nature Conservation, and Nuclear Safety of Germany within the KaLiPat project. G.A.E., D.B., B.S., S.P., and J.H. acknowledge the financial support of BMW AG.

REFERENCES

(1) Scrosati, B.; Garche, J. Lithium Batteries: Status, Prospects and Future. *J. Power Sources* **2010**, *195*, 2419−2430.
(2) Kraytsberg, A.; Ein-Eli, Y. Higher, Stronger, Better··· A Review of 5 V Cathode Materials for Advanced Lithium-Ion Batteries. *Adv. Energy Mater.* **2012**, *2*, 922−939.
(3) Scrosati, B.; Hassoun, J.; Sun, Y.-K. Lithium-ion Batteries. A Look Into the Future. *Energy Environ. Sci.* **2011**, *4*, 3287−3295.
(4) Ellis, B. L.; Town, K.; Nazar, L. F. New Composite Materials for Lithium-ion Batteries. *Electrochim. Acta* **2012**, *84*, 145−154.
(5) Zhang, W. M.; Hu, J. S.; Guo, Y.; Zheng, S. F.; Zhong, L. S.; Song, W. G.; Wan, L. J. Tin-Nanoparticles Encapsulated in Elastic Hollow Carbon Spheres for High-Performance Anode Material in Lithium-Ion Batteries. *Adv. Mater.* **2008**, *20*, 1160−1165.
(6) Guo, B.; Shu, J.; Tang, K.; Bai, Y.; Wang, Z.; Chen, L. Nano-Sn/hard Carbon Composite Anode Material With High-initial Coulombic Efficiency. *J. Power Sources* **2008**, *177*, 205−210.
(7) Dou, S. Review and Prospect of Layered Lithium Nickel Manganese Oxide as Cathode Materials for Li-ion Batteries. *J. Solid State Electrochem.* **2013**, *17*, 911−926.
(8) Jarvis, K. A.; Deng, Z.; Allard, L. F.; Manthiram, A.; Ferreira, P. J. Understanding Structural Defects in Lithium-rich Layered Oxide Cathodes. *J. Mater. Chem.* **2012**, *22*, 11550−11555.
(9) Johnson, C. S.; Li, N.; Lefief, C.; Vaughey, J. T.; Thackeray, M. M. Synthesis, Characterization and Electrochemistry of Lithium Battery Electrodes: $xLi_2MnO_3\cdot(1-x)LiMn_{0.333}Ni_{0.333}Co_{0.333}O_2$ ($0 < x < 0.7$). *Chem. Mater.* **2008**, *20*, 6095−6106.
(10) Li, J.; Klöpsch, R.; Stan, M. C.; Nowak, S.; Kunze, M.; Winter, M.; Passerini, S. Synthesis and Electrochemical Performance of the High Voltage Cathode material Li[$Li_{0.2}Mn_{0.56}Ni_{0.16}Co_{0.08}$]$O_2$ with improved rate capability. *J. Power Sources* **2011**, *196*, 4821−4825.
(11) Wang, J.; He, X.; Paillard, E.; Liu, H.; Passerini, S.; Winter, M.; Li, J. Improved Rate Capability of Layered Li-Rich Cathode for Lithium Ion Battery by Electrochemical Treatment. *ECS Electrochem. Lett.* **2013**, *2*, A78−A80.
(12) Hassoun, J.; Lee, K.-S.; Sun, Y.-K.; Scrosati, B. An Advanced Lithium Ion Battery Based on High Performance Electrode Materials. *J. Am. Chem. Soc.* **2011**, *133*, 3139−3143.

(13) Derrien, G.; Hassoun, J.; Panero, S.; Scrosati, B. Nanostructured Sn−C Composite as an Advanced Anode Material in High-Performance Lithium-Ion Batteries. *Adv. Mater.* **2007**, *19*, 2336−2340.
(14) Hassoun, J.; Derrien, G.; Panero, S.; Scrosati, B. A Nanostructured Sn−C Composite Lithium Battery Electrode with Unique Stability and High Electrochemical Performance. *Adv. Mater.* **2008**, *20*, 3169−3175.
(15) Li, J.; Zheng, J. M.; Yang, Y. The Studies on Storage Characteristics of $LiNi_{0.4}Co_{0.2}Mn_{0.4}O_2$ as a cathode material in lithium ion batteries. *J. Electrochem. Soc.* **2007**, *154*, A427−A432.
(16) Boulineau, A.; Croguennec, L.; Delmas, C.; Weill, F. Structure of Li_2MnO_3 With Different Degrees of Defects. *Solid State Ionics* **2010**, *180*, 1652−1659.
(17) Song, B.; Liu, Z.; Lai, M. O.; Lu, L. Structural Evolution and the Capacity Fade Mechanism Upon Long-term Cycling in Li-rich Cathode Material. *Phys. Chem. Chem. Phys.* **2012**, *14*, 12875−12883.
(18) Zhang, X.; Jiang, W. J.; Mauger, A.; Qilu, F.; Gendron, C. M. Julien; Minimization of the Cation Mixing in $Li_{1+x}(NMC)_{1-x}O_2$ as Cathode Material. *J. Power Sources* **2010**, *195*, 1292−1301.
(19) Peng, Q. W.; Tang, Z. Y.; Zhang, L. Q.; Li, X. J. Synthesis of Layered $Li_{1.2+x}[Ni_{0.25}Mn_{0.75}]_{0.8-x}O_2$ Materials ($0 \leq x \leq 4/55$) Via a New Simple Microwave Heating Method and their Electrochemical Properties. *Mater. Res. Bull.* **2009**, *44*, 2147−2151.
(20) Winter, M.; Besenhard, J. O.; Spahr, M. E.; Novák, P. Insertion Electrode Materials for Rechargeable Lithium Batteries. *Adv. Mater.* **1998**, *10*, 725−763.
(21) Wen, C. J.; Huggins, R. A. Thermodynamic Study of the Lithium-Tin System. *J. Electrochem. Soc.* **1981**, *128*, 1181−1187.
(22) Hassoun, J.; Wachtler, M.; Wohlfahrt-Mehrens, M.; Scrosati, B. Electrochemical Behaviour of Sn and Sn−C Composite Electrodes in LiBOB Containing Electrolytes. *J. Power Sources* **2011**, *196*, 349−354.
(23) Kim, J. S.; Johnson, C. S.; Vaughey, J. T.; Thackeray, M. M. Hackney, S.A.; Electrochemical and Structural Properties of $xLi_2M'O_3 \cdot (1-x)LiMn_{0.5}Ni_{0.5}O_2$ Electrodes for Lithium Batteries (M′ = Ti, Mn, Zr; 0 ≤ x 0.3). *Chem. Mater.* **2004**, *16*, 1996−2006.
(24) Yabuuchi, N.; Yoshii, K.; Myung, S.-T.; Nakai, I.; Komaba, S. Detailed Studies of a High-Capacity Electrode Material for Rechargeable Batteries, Li_2MnO_3−$LiCo_{1/3}Ni_{1/3}Mn_{1/3}O_2$. *J. Am. Chem. Soc.* **2011**, *133*, 4404−4419.
(25) Park, S.-H.; Kang, S.-H.; Johnson, C. S.; Amine, K.; Thackeray, M. M. Lithium−Manganese−Nickel-Oxide Electrodes with Integrated Layered−Spinel Structures for Lithium Batteries. *Electrochem. Commun.* **2007**, *9*, 262−268.
(26) Johnson, C. S.; Li, N.; Vaughey, J. T.; Thackeray, M. M. Lithium−Manganese Oxide Electrodes With Layered−Spinel Composite Structures xLi_2MnO_3 $(1-x)Li_{1+y}Mn_{2-y}O_4$ ($0 < x < 1$, 0 6 y 6 0.33) for Lithium Batteries. *Electrochem. Commun.* **2005**, *7*, 528−536.
(27) Chae, C.; Noh, H.-J.; Lee, J. K.; Scrosati, B.; Sun, Y.-K. A High-Energy Li-Ion Battery Using a Silicon-Based Anode and a Nano-Structured Layered Composite Cathode. *Adv. Funct. Mater.* **2014**, *24*, 3036−3042.